Biophysical Chemistry 22 (1985) 53–64
Elsevier

BPC 00923

THE EFFECT OF HISTONE H1 ON THE COMPACTION OF OLIGONUCLEOSOMES

A QUASIELASTIC LIGHT SCATTERING STUDY

Christian MARION [a], Christine HESSE-BEZOT [c], Pierre BEZOT [c], Marie-Jeanne MARION [b], Bernard ROUX [a] and Jean-Claude BERNENGO [d]

Laboratoires de [a] Physico-Chimie Biologique et de [b] Biochimie Médicale, Université Claude Bernard, 69622 Villeurbanne Cedex and Laboratoires de [c] Physique de la Matière Condensée et de [d] Biophysique, Université de Nice, 06034 Nice, France

Received 22nd August 1984
Revised manuscript received 20th January 1985
Accepted 20th January 1985

Key words: Oligonucleosome structure; Histone H1; Circular dichroism; Dynamic light scattering; Thermal denaturation

The structural properties of H1-depleted oligonucleosomes are investigated by the use of quasielastic laser light scattering, thermal denaturation and circular dichroism and compared to those of H1-containing oligomers. To obtain information on the role of histone H1 in compaction of nucleosomes, translational diffusion coefficients (D) are determined for mono-to octanucleosomes over a range of ionic strength. The linear dependences of D on the number of nucleosomes show that the conformation of stripped oligomers is very extended and does not change drastically with increasing the ionic strength while the rigidness of the chain decreases due to the folding of linker DNA. The results prove that the salt-induced condensation is much smaller for H1-depleted than for H1-containing oligomers and that histone H1 is necessary for the formation of a supercoiled structure of oligonucleosomes, already present at low ionic strength.

1. Introduction

A better knowledge of the relative spatial arrangement of the linker DNA with respect to adjacent nucleosomes should provide useful information for understanding the structural organization of chromatin (for recent reviews, see refs. 1 and 2). The nucleosome filament that constitutes the first level of packing of DNA in chromatin is further folded into a fiber of 25–30 nm in diameter in nuclei and in isolated chromosomes [3–7]. This fiber has been interpreted either as helically organized repeating nucleosomal units [8] or, alternatively, as repeating clusters of nucleosomes or 'superbeads' [9]. It is now widely accepted that histone H1 is required for condensation of polynucleosomes into the 30 nm fiber [8–12]. Histone H1 thus interacts with chromatin on all the levels of DNA packing since the stabilization of the two turns of nucleosomal DNA [11,13] as well as the precipitation of chromatin and the condensation of chromatin in nuclei [14–16] are dependent on H1.

One way to contribute to the resolution of problems of spatial arrangement of nucleosomes and final folding of chromatin as well as the role of H1 is to study physical properties of oligonucleosomes. Several authors have already attempted to investigate the conformation of nucleosomal chains by hydrodynamic methods such as sedimentation, neutron and light scattering or electric dichroism and birefringence. However, in many studies the preparations used were heterogeneous in molecular weight. We have eliminated this problem by studying lower-order oligomers containing up to eight nucleosomes and which can be obtained as purified homogeneous samples [17–24].

In previous papers, we reported transient elec-

tric birefringence [17–19,22–24] and quasielastic light scattering [20,21] studies of rat liver chromatin oligomers with their full complement of histone H1. The results showed a change in conformation with the hexamer and that has been confirmed by sedimentation data [25–27]. By comparing the conformation of H1-containing oligonucleosomes with that of oligomers stripped of H1, we can investigate the role of H1 in packaging nucleosomes in the chains. We have shown that the transition in electro-optical behavior at six nucleosomes disappears when H1 is removed from oligonucleosomes by treatment with an ion-exchange resin [28] and the negative electric birefringence becomes proportional to the nucleosomal chain length [19,24]. The observed alterations are explained by an unfolding of the H1-depleted oligomers with the appearance of extended 'bead and bridge' structures. We have supplemented these data with quasielastic light scattering measurements which are particularly suitable to reveal overall differences in the size and shape of chromatin particles [29–36].

In the present study, we examined the involvement of histone H1 in the folding of low-order oligonucleosomes by carrying out in parallel dynamic light scattering, circular dichroism and thermal denaturation studies.

2. Materials and methods

2.1. Isolation of nuclei and chromatin

Nuclei were isolated from rat liver as described by Hewish and Burgoyne [37] and washed repeatedly in 0.34 M sucrose in buffer A (15 mM Tris-HCl, pH 7.4, 60 mM KCl, 15 mM NaCl, 0.15 mM spermine, 0.5 mM spermidine, 15 mM β-mercaptoethanol) until they were free of cytoplasmic debris as judged by phase-contrast microscopy. Nuclei were diluted to a concentration of 2×10^8 nuclei/ml and incubated for 10 min at 37°C in the presence of 1 mM $CaCl_2$. Chromatin was solubilized by digestion with micrococcal nuclease (Worthington, 200 U/ml) for 2 min 30 s. The reaction was terminated by adding EDTA to a final concentration of 5 mM and chilling on ice. Nuclei were then lysed in 0.2 mM EDTA, pH 7.0, 0.2 mM $PhMeSO_2F$. After centrifugation the chromatin was recovered in the supernatant and 60–80 A_{260} units were layered on an isokinetic sucrose gradient (5–28.2%; 1 mM phosphate buffer, pH 7.4, 1 mM EDTA) according to Finch et al. [38]. After 19 h centrifugation at 26000 rpm in a Beckman SW 27 rotor, nucleosome oligomers comprising up to eight consecutive nucleosomes can be separated and analyzed using a Gilford density gradient scanner [21,24]. Fractions corresponding to each peak were pooled and dialysed overnight against 1 mM phosphate buffer, pH 7.4, 0.2 mM EDTA.

2.2. Preparation of H1-depleted oligonucleosomes

Histone H1 was selectively removed from oligonucleosomes by treatment with the ion-exchange resin AG 50W-X2. Equal amounts of native oligonucleosomes in 1 mM phosphate buffer, pH 7.4, 0.2 mM EDTA and buffer solution containing 900 mM NaCl were mixed under gentle stirring. 0.2 ml of sedimented resin/ml (≈ 10 A_{260} units chromatin) was then added to the solutions of chromatin. The resin was preparated by the procedure of Bolund and Johns [28] and equilibrated with 1 mM sodium phosphate buffer, pH 7.4, 0.2 mM EDTA and the appropriate NaCl concentration.

After gently stirring for 1 h at 4°C, the samples were centrifuged at $800 \times g$ for 5 min. The supernatants containing H1-depleted oligomers were then dialyzed overnight at 4°C against 1 mM phosphate buffer, pH 7.4, and 0.2 mM EDTA for physical measurements.

2.3. Characterization of oligonucleosomes

2.3.1. DNA extraction and electrophoresis

DNA was prepared by removal of proteins via overnight digestion with 0.1 mg proteinase K/ml (Merck) in 1 M NaCl, 1% SDS, 3 mM EDTA at 37°C followed by two extractions with an equal volume of phenol-chloroform-isoamyl alcohol (25:24:1) and three extractions with chloroform-isoamyl alcohol (24:1). DNA in the aqueous phase was then precipitated with 2 vols. of absolute ethanol at −20°C, collected by centrifugation and

dissolved in gel buffer (36 mM Tris-HCl, pH 7.7, 30 mM NaH_2PO_4, 1 mM EDTA, 0.2% SDS).

The DNA from oligonucleosomes was analyzed on tube gels with a 2.4–8.5% linear polyacrylamide gradient. Polyacrylamide solutions were according to Loening [39]. Bromphenol blue was used as a mobility marker and the calibration of the gels was made with *Hae*III restriction fragments of ϕX 174 DNA. At the end of the electrophoresis, the gels were removed from the tubes, rinsed with distilled water and their absorbance at 260 nm was recorded using a 250 Gilford spectrophotometer with gel scanning accessory.

2.3.2. Protein analysis

Histones were extracted twice with 0.25 N HCl (final concentration) under fast vortex mixing and recovered by sedimentation of precipitated DNA. The supernatant was extensively dialyzed against distilled water and lyophilized. Histones were then dissolved in 0.9 N acetic acid and 15% sucrose and analyzed on acid-urea 15% acrylamide gels as described by Panyim and Chalkley [40]. Gels were stained with 0.1% Coomassie blue in 40% methanol and 10% acetic acid, destained in 10% methanol and 7% acetic acid and scanned at 550 nm.

2.4. Spectroscopic analysis

Absorption spectra were recorded on Gilford 250 spectrophotometer. Circular dichroism (CD) measurements were made at room temperature with a Roussel-Jouan, Mark III dichrograph (Jobin-Yvon). Concentrations of DNA nucleotide residues in whole and H1-depleted oligonucleosomes were determined by the absorption at 260 nm using an extinction coefficient of 6600 cm^{-1} (mol nucleotide)$^{-1}$. Samples used were about 1.5 $\times 10^{-4}$ M nucleotide residue in 1 mM phosphate buffer, pH 7.4, 0.2 mM EDTA. The results are presented in terms of molar ellipticity, $|\theta|$, in degree cm^2 $dmol^{-1}$. CD spectra were recorded in the range 250–320 nm in cylindrical cuvettes with 1 cm optical path length.

2.5. Thermal denaturation measurements

Chromatin samples were thermally denatured in 1.0 mM phosphate buffer, pH 7.4, 0.2 mM EDTA at A_{260} (25°C) $\approx$ 0.8–1.0. Samples were placed in quartz cuvettes with 1 cm path length, carefully degassed and sealed with a Teflon stopper.

Denaturation profiles were recorded in a 250 Gilford spectrophotometer connected to a 2527 Gilford thermoprogrammer. Normally, a starting temperature of 25°C and a heating rate of 0.5°C/min were used and a final temperature in the cuvette of about 95°C was achieved. The correction for thermal expansion was automatically made with a Gilford model 2535 reference compensator.

The percent hyperchromicity at temperature T is defined as

$$h = \frac{A_{260}^{T} - A_{260}^{25°C}}{A_{260}^{25°C}} \times 100 \quad (1)$$

where A_{260}^{T} is the absorbance at wavelength 260 nm and temperature T (°C) and $A_{260}^{25°C}$ is the absorbance at 260 nm and 25°C (the base temperature).

The transition midpoint, t_m, is defined as the temperature of maximum dh/dt for each thermal transition.

2.6. Quasielastic polarized light scattering experiments

The experimental setup has already been described elsewhere [41]. The measurements are carried out in an optical thermostatted cell (19°C) after ultracentrifugation of the solution samples and the scattered light intensity is analyzed at 90° scattering angle. The exciting source is a vertically polarized argon ion laser ($\lambda = 5145$ Å). The polarized light scattered by the molecules interferes with an intense reference beam (heterodyne technique), and the measured spectrum is directly related to the first-order electric field correlation function $g^{(1)}(t)$. For a solution containing n macromolecules of different shapes and sizes, $g^{(1)}(t)$ is given by

$$g^{(1)}(t) = \sum_{i=1}^{n} a_i e^{-t/\tau_i} \quad (2)$$

where τ_i is the relaxation time related to the

translational diffusion coefficient D_i of species i by

$$\tau_i = 1/q^2 D_i \quad (3)$$

q is the scattering vector defined as

$$q = (4\pi n/\lambda_0)\sin(\phi/2) \quad (4)$$

where n is the solution refractive index, λ_0 the laser wavelength in vacuo and ϕ the scattering angle. It should be pointed out that eq. 2 is only valid if the length of all the molecules remains smaller than $\lambda/10$.

The friction factor was then obtained from the Einstein relationship

$$f_i = kT/D_i \quad (5)$$

where k is Boltzmann's constant and T the absolute temperature.

To obtain the maximum information over a large time range, the photocurrent autocorrelation function was recorded for four different sampling times.

The corresponding correlation functions are matched and fitted to three theoretical curves representing a unimodal, Gaussian unimodal and bimodal distribution by means of a 'conjugated' gradient algorithm. According to a least-squares criterion, the bimodal distribution always fits significantly better, and all the values reported here have been obtained in that way.

3. Results and discussion

3.1. Preparation and characterization of chromatin oligomers

Chromatin oligomers are obtained by sedimentation of nuclease digested chromatin through isokinetic sucrose gradients as described previously [17]. Fig. 1 shows 2.4–8.5% polyacrylamide gel gradient electrophoresis of DNA extracted from collected fractions. The nucleosomal repeat length, as calculated from these gels with *Hae*III restriction fragments of ϕX 174 DNA, is found to be the same in all oligomers, 194 ± 4 base-pairs (table 1). Electrophoretic profiles and electron microscopic observations (data not shown) show the high degree of purity of samples. This confirms the electric birefringence results showing perfect monoexponential decays for H1-containing oligomers [17,24].

The removal of histone H1, as judged by acid-urea/polyacrylamide gel electrophoresis, was complete at 450 mM NaCl, 1 mM sodium phosphate buffer, pH 7.4, in the presence of the ion-exchange resin (fig. 2). No measurable loss of the four core histones is observed and the absence of additional bands shows that no proteolytic degradation occurred during the preparation procedure.

3.2. Circular dichroism and thermal denaturation experiments

The effect of removal of H1 is studied by CD and thermal denaturation profiles. Using these techniques, intact and H1-stripped oligomers are examined and compared in 1 mM phosphate buffer, pH 7.4, 0.2 mM EDTA (tables 1 and 2).

Above 250 nm, the CD spectrum is a sensitive probe of DNA conformational change, since it is entirely due to the DNA component. The spectra of native oligomers exhibit a positive peak at 282 nm with a shoulder at 274 nm and a negative peak at 296 nm (fig. 3). The results presented in terms of molar ellipticity $|\theta|$ ($|\theta|_{282} = 1930 \pm 300$ degree cm^2 dmol^{-1}; $|\theta|_{274}/|\theta|_{282} = 0.72 \pm 0.02$) are in good agreement with previous reports [42–44]. Removal of H1 caused marked changes in the CD spectra: the molar ellipticity values are sharply increased with a higher $|\theta|_{274}/|\theta|_{282}$ ratio, the negative peak around 296 nm disappears and the crossover (zero ellipticity) point shifts from 268 to 262 nm.

The absorbance melting profile of DNA indicates its degree of stabilization by proteins. Profiles of native oligomers were found to be mainly monophasic, showing a very high cooperativity with $t_m = 79.5 \pm 0.3$°C and hyperchromicity $h = 40.5 \pm 0.5\%$. A typical thermal denaturation of H1-depleted oligomers plotted as the relative hyperchromicity vs temperature is shown in fig. 4. This represents a biphasic melting profile. The first transition had $t_{m1} = 52$°C while the main transition, with $t_{m2} = 75$°C, represents approx. 45%

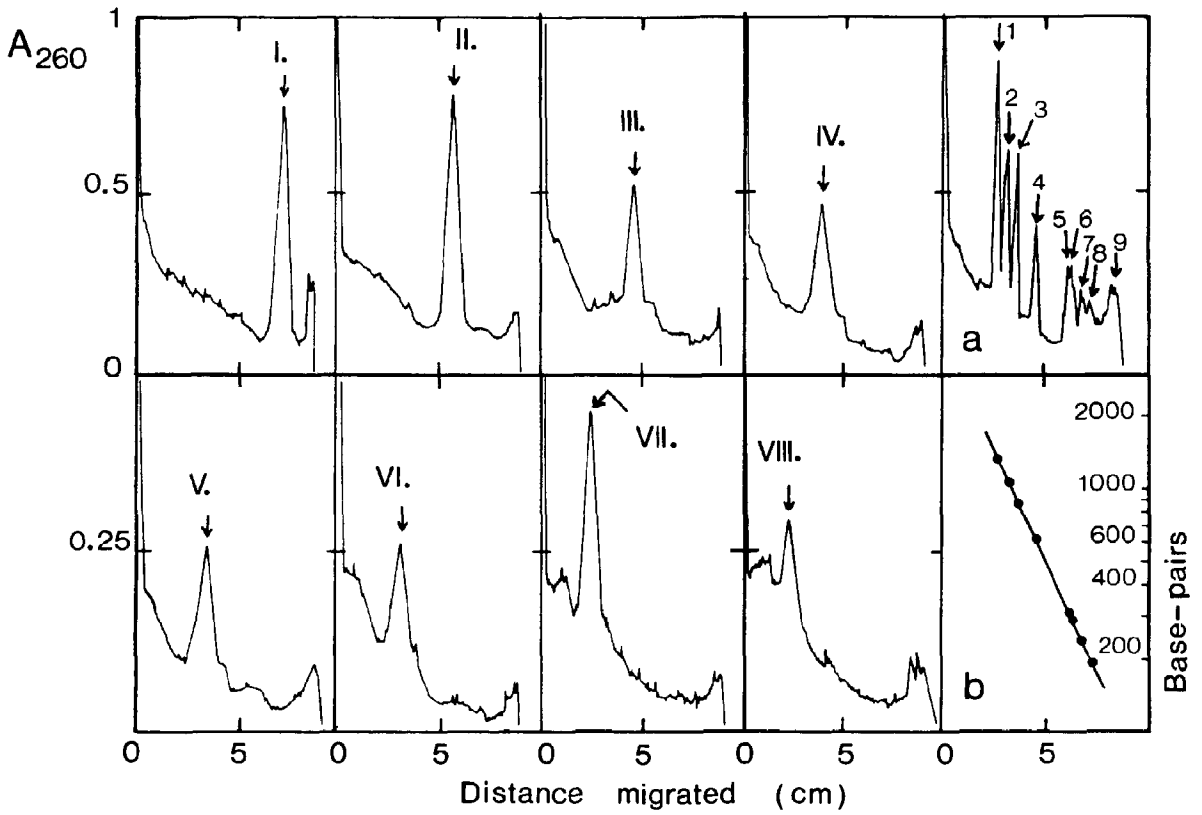

Fig. 1. DNA gel-electrophoresis profiles of oligonucleosomes. The reference number of each oligomer sample is indicated on each profile. The reference peaks of the ΦX 174 DNA digested by *Hae*III (a) correspond to fragments of 1342, 1078, 872, 606, 310, 278, 234 and 194 base-pairs (b). Peak 9 corresponds to bromophenol blue.

Table 1

DNA lengths, transition temperatures and hyperchromicities of oligonucleosomes

DNA lengths were determined from oligonucleosome DNA electrophoretic mobility on 2.4–8.5% polyacrylamide tube gels. The calibration of the gels was made with *Hae*III restriction fragments of ϕX 174 DNA. Thermal denaturation was performed in 1 mM sodium phosphate buffer, pH 7.4, 0.2 mM EDTA. T_m, T_{m1}, T_{m2} are the temperatures of maximum dh/dT for each transition, h_T the total hyperchromicity and h_1 the hyperchromicity found in the first transition for H1-depleted oligomers.

Chromatin subunit	DNA length (base-pairs)	Native oligomers		H1-depleted oligomers		
		T_m (°C)	h_T (%)	T_{m1} (°C)	T_{m2} (°C)	h_1/h_T
Monomer	194	79	40.7	52	75	0.58
Dimer	380	79.5	40	52	75.5	0.54
Trimer	590	79.5	41.5	52	75	0.54
Tetramer	780	79	41	51.5	74	0.56
Pentamer	990	80	41.8	52	75	0.54
Hexamer	1155	79.5	40.6	53	76	0.56
Heptamer	1380	80	41.1	52	74.5	0.53
Octamer	1510	79	41	52.5	75.5	0.51
Mean value	194	79.5	41	52.1	75	0.55
Deviation	2–3%	±0.5	±0.8	±0.8	±1.0	±0.04

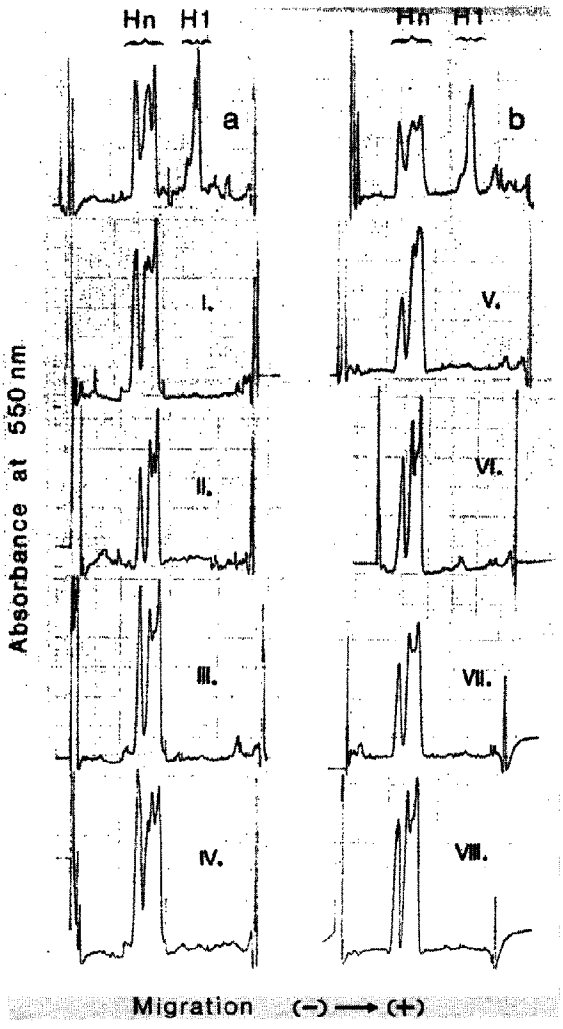

Fig. 2. Densitometric scans of histones extracted from oligonucleosomes after the removal of H1. The reference number of each oligomer sample is indicated on each profile. a and b show the profiles of histones extracted from native mononucleosomes (a) and octanucleosomes (b).

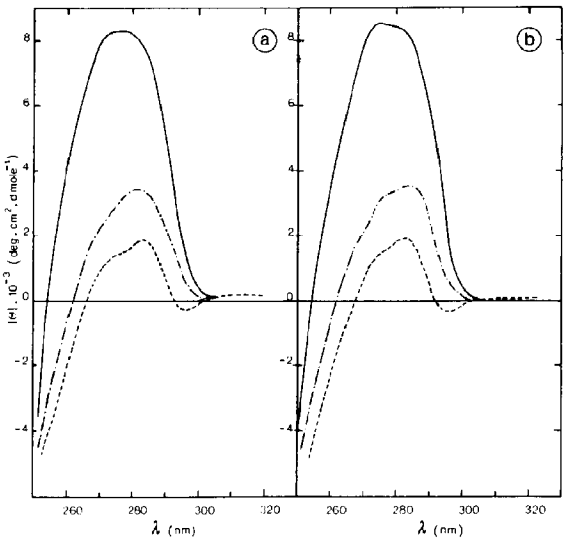

Fig. 3. Circular dichroism spectra of mononucleosomes (a) and octanucleosomes (b). (------) Native oligomers, (·–·–·) H1-depleted oligomers and (———) DNA extracted. Solvent: 1 mM sodium phosphate buffer, 0.2 mM EDTA, pH 7.4.

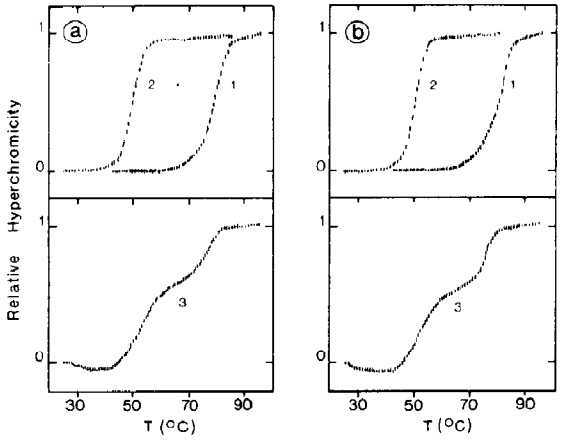

Fig. 4. Thermal denaturation profiles of mononucleosomes (a) and octanucleosomes (b). (1) Native oligomers, (2) DNA extracted and (3) H1-depleted oligomers. Solvent: 1 mM sodium phosphate buffer, 0.2 mM EDTA, pH 7.4.

of the total hyperchromicity change. Although the linker becomes more sensitive to thermal denaturation, it is still stabilized by proteins since it melts at 4°C higher than pure DNA in the same buffer (fig. 4). On the other hand, the loss of H1 causes a decrease in the main transition of 4.5°C.

In several studies, results different from ours have been reported, native samples having higher ellipticity $|\theta|_{283}$ values ($\approx$ 4000 degree cm^2 dmol^{-1}) and exhibiting neither negative peaks around 295 nm in CD spectra nor monophasic

Table 2

Circular dichroism parameters of rat liver oligonucleosomes

Circular dichroism spectra were recorded in 1 mM sodium phosphate buffer, pH 7.4, 0.2 mM EDTA. Molar ellipticities were calculated on the basis of DNA nucleotide concentration. The values of the crossover (zero ellipticity) points λ_0 are to the nearest 1.0 nm.

Chromatin subunit	Native oligomers			H1-depleted oligomers		
	$\lvert\theta\rvert_{282}$ (degree cm^2 dmol^{-1})	$\lvert\theta\rvert_{275}/\lvert\theta\rvert_{282}$	λ_0 (nm)	$\lvert\theta\rvert_{282}$ (degree cm^2 dmol^{-1})	$\lvert\theta\rvert_{275}/\lvert\theta\rvert_{282}$	λ_0 (nm)
Monomer	1950	0.72	267	3400	0.86	263
Dimer	2050	0.74	268	3520	0.88	262
Trimer	2080	0.69	269	3780	0.87	261
Tetramer	1940	0.72	268	3670	0.88	262
Pentamer	2100	0.70	268	3775	0.87	262
Hexamer	1780	0.71	269	3725	0.87	262
Heptamer	2030	0.74	267	3700	0.88	261
Octamer	1850	0.72	268	3630	0.90	260
Mean value	1970	0.72	268	3650	0.88	262
Deviation	±200	±0.02	±1	±250	±0.02	±2

denaturation profiles [45–49].

The CD spectra observed by Fasman et al. do actually correspond to sheared damaged [42] or protein-depleted chromatin and, in view of this fact, the molar ellipticity of 4000 and multiphasic profiles are consistent with our results. The data reported by these authors may result from unfolding of oligomeric structures mainly due to the method of preparation used (gel filtration). Recall that only a small length of residual linker increases the ellipticities greatly, especially at low ionic strength [50].

Fasman et al. [47,48] have, however, suggested that the low ellipticity values found for oligonucleosomes or chromatin (≈ 2000 degree cm^2 dmol^{-1}) were due to additional tertiary folding of the linker region. The linker DNA in low-ellipticity chromatin would thus be probably condensed in a similar manner to that of core DNA. This proposition was based on data showing CD spectra of chromatin similar to those for core particles which contain little linker DNA and assuming that the higher-order folding of chromatin contributes to the CD spectrum in a significant way. It appears that several lines of evidence speak against such an explanation for the low ellipticity values of oligonucleosomes and chromatin. Firstly, detailed CD studies [50,51] show that the core particle has an ellipticity maximum of $|\theta|_{282} = 1300$ degree cm^2 dmol^{-1} at low ionic strength. A maximum of 2000 degree cm^2 dmol^{-1} is only found when core particle is destabilized in 0.6 M NaCl [51]. Secondly, the results presented here clearly confirm that at room temperature the superstructure of chromatin does not contribute to the CD signal [42], since the $|\theta|_{282}$ values for oligonucleosomes are the same as that obtained for native chromatin under similar ionic conditions [52–54]. Thirdly, it is well-established that oligo- and polynucleosomes exhibit extended structures at the low ionic strength we use (1 mM sodium phosphate). The linker region can then be further condensed when the fibers gradually fold up into the solenoid of pitch 11 nm [8]. A folding of linkers, already existing at low salt concentration, seems therefore to be unrealistic.

3.2. *Quasielastic light-scattering measurements*

Quasielastic light scattering experiments were performed on H1-depleted oligomers in 1 mM sodium phosphate buffer, pH 7.4, 0.2 mM EDTA with increasing ionic strength (NaCl). To avoid problems due to interference from aggregation and dust particles, buffers and chromatin samples were centrifuged for 1 h at 200 000 × g before the mea-

surements. Solution concentrations were taken in the range 0.3–3 A_{260} after preliminary experiments which have shown the independence of relaxation times from concentration in this range. The experimental angle of scattering is 90°. No angular dependence in the evaluation of D was observed for nucleosome [33,36] or short chains of chromatin [56].

Actually, taking into account the precision of our experiments, $g^{(1)}(t)$ can be approximated by a sum of only two exponential terms: the nucleosome oligomer (subscript 1) and high-order aggregates which are impossible to eliminate completely (subscript 2).

$$g^{(1)}(t) = a_1 e^{-t/\tau_1} + (1 - a_1) e^{-t/\tau_2} \quad (6)$$

The relaxation time τ_1, from which the translational diffusion coefficient D is calculated, contributes about 55–80% to the relaxation mechanism. This shows that H1-depleted samples are far less monodisperse than the native ones which exhibited contributions of about 70–95% [20,21]. For H1-depleted oligomers the measurements were repeated on three different preparations at an interval of several months. Although the standard deviations of fast relaxation times (about 8–12%, judged from the spacing of data) are larger than those observed for native oligomers [21], we are confident in the overall effect reported here.

For oligomers in solutions with salt concentration varying between 0 and 80 mM NaCl, the relaxation times are summarized in table 3. The dependencies of translational coefficients on the number of nucleosomes in the chain (n) are presented in fig. 5a. The double-logarithmic plots of

$$D = k_D n^b \quad (7)$$

are linear and we can estimate the effect of increasing ionic strength from the values of b.

For oligomers without H1 at low ionic strength (1 mM phosphate buffer, pH 7.4, 0.2 mM EDTA) the experimental data are described by the relation

$$D = 1.95 \times 10^{-7} n^{-0.65} \quad (8)$$

When 80 mM NaCl is added, the experimental data are plotted on a straight line with a slightly lower slope (fig. 5b) and are described by the equation

$$D = 2.32 \times 10^{-7} n^{-0.60} \quad (9)$$

3.3. *Conformation of H1-depleted oligonucleosomes at low ionic strength*

The value of the exponent b in the expression for the dependence on D of n may characterize

Table 3

Quasielastic light scattering measurements on H1-depleted oligonucleosomes

Quasielastic light scattering experiments were performed in 0.2 mM EDTA, 1 mM phosphate buffer, pH 7.4, on solutions with A_{260} in the range 0.3–3. The relaxation times τ for the autocorrelation functions were obtained by using a bimodal distribution fitting ($a_2 = 1 - a_1$). The measurements have been repeated on three different preparations at intervals of several months with standard deviation of fast relaxation times ±8–12%.

Chromatin subunit	Ionic strength								
	Without NaCl			20 mM NaCl			80 mM NaCl		
	a_1	τ_1 (μs)	τ_2 (ms)	a_1	τ_1 (μs)	τ_2 (ms)	a_1	τ_1 (μs)	τ_2 (ms)
Monomer	0.58	95	1.31	0.75	87	1.10	0.80	72	1.19
Dimer	0.67	168	1.00	0.77	144	1.40	0.75	130	1.44
Trimer	0.72	195	2.17	–	–	–	0.76	162	0.71
Tetramer	0.73	237	2.02	0.69	217	3.26	0.72	235	2.83
Pentamer	0.65	259	1.54	0.65	218	1.62	0.64	216	1.95
Hexamer	0.59	257	1.25	0.60	255	2.65	0.62	250	2.44
Heptamer	0.50	279	1.46	0.73	266	1.51	0.81	286	2.51
Octamer	0.57	370	2.25	0.73	295	2.62	0.75	278	1.95

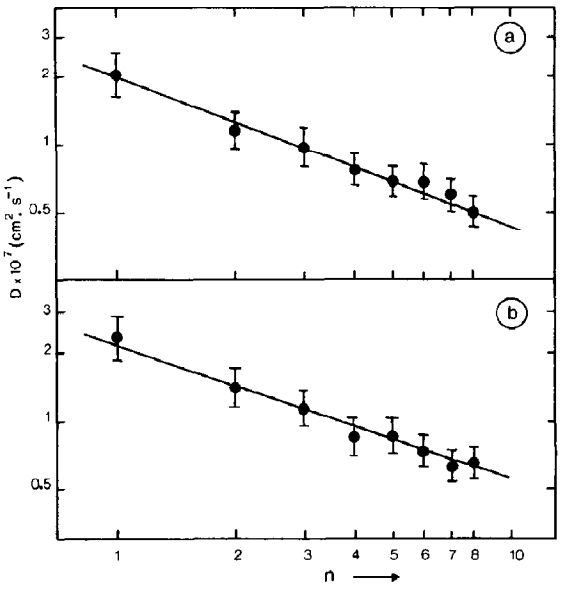

Fig. 5. Dependence of translational diffusion coefficient on the number of nucleosomes with 80 mM (b) and without (a) NaCl in 0.2 mM EDTA, 1 mM sodium phosphate buffer, pH 7.4.

the degree of compaction and permeability of the polymer chain [57]. b varies from -0.35 for solid spheres to -0.80 for very long rods with axial ratios higher than 100. b is related to the exponent of the molecular weight power dependence of the sedimentation coefficient, i.e.

$$s = kn^a \tag{10}$$

by the relation

$$(a - b) = 1 \tag{11}$$

At low salt concentration, H1-containing oligonucleosomes present a change in the power-law relationship: $D \propto n^b$ between hexamer and heptamer [21] which is not observed here with H1-stripped oligonucleosomes. This discontinuity, also observed in sedimentation measurements [25–27], is consistent with the formation of a unit of higher-order structure and suggests that a well-defined organization exists in low salt conditions. Static [58] and dynamic [30–32] light scattering, neutron scattering [59], electric birefringence [17,18,24,55] and recently synchrotron radiation X-ray scattering [60] also provide evidence that this superstructure reflects the same solenoidal or helical form observed at higher ionic strength for the condensed '30 nm fiber' with approximately the same outer diameter but with a greater pitch.

The value of b which we observed for H1-depleted oligonucleosomes ($b = -0.65$) is in good agreement with sedimentation data obtained in similar ionic conditions: $a = 0.36$ [61], 0.41 [62] and 0.43 [23] and indicates a relatively high unfolding of the nucleosomal chain without discontinuity in behavior. We recall that we have found a value of $b = -0.51$ for native oligomers [21]. Our transient electric birefringence results confirm the absence of any transition after the removal of H1 [19,24]: the steady-state birefringence as well as the orientational relaxation time regularly increase with the number of nucleosomes in the chain. On the other hand, both the analysis of rise and decay areas and bipolar pulse experiments show that H1-stripped oligomers orient themselves in an electric field by an induced dipole mechanism. All these results indicate that oligonucleosomes are highly extended because of the unwinding of DNA tails and internucleosomal segments. Each segment behaves like free DNA and the faces of the nucleosome discs are more or less parallel to the filament axis [24].

On the other hand, the transition in the structure of oligonucleosomes produced by the removal of H1 has been observed by electron microscopy. Oligomers appear as 'beads-on-a-string' with the nucleosomes separated from each other by distances of about 150–200 Å (data not shown). However, our experimental conditions for the removal of H1 are mild enough and do not induce any marked histone redistribution with sliding of nucleosomes and/or linearization with opening out of nucleosomes [11]. The higher ellipticity values and the biphasic nature of the melting curve of H1-depleted oligomers confirm that the DNA is not uniformly stabilized in this chromatin and are in agreement with the presence of free-DNA-like regions. The molar ellipticity $|\theta|$ at 282 nm is 3650 degree cm^2 dmol^{-1} instead of 1970 for H1-containing oligomers at low ionic strength (table 2). This can be explained by the contribution of about 52 base-pairs of naked DNA (by assuming a molar ellipticity value of 8300 for DNA).

Such a result is consistent with the De la Torre and Bloomfield modelisation which has been previously applied to interpret our experimental results in the presence of H1 [20,21]. The lollipop model [63] was used to explain the shape of the monomer and the dimensions are reasonably well in accordance with electron micrographs. The radius σ_1 of the spherical head and the radius σ_2 of the hydrated DNA tail were taken as 55 and 12.5 Å, respectively. Keeping σ_1/σ_2 constant, the length L of the tail was calculated from the values of translational diffusion coefficients D. The decrease in D from 3.02×10^{-7} cm^2 s^{-1} [21] to 2.16×10^{-7} cm^2 s^{-1} with the removal of histone H1 is consistent with an increase in the tail length of about 230 Å, corresponding to an average of 68 base-pairs. Such an unwinding of internucleosomal segments explains the highly extended structure observed for oligonucleosomes, as shown by the value of b (-0.65), very close to that obtained for long rods.

3.4. Effect of histone H1 on the compaction of oligonucleosomes

To determine the function of H1 in the salt-induced conformational changes shown previously [21], the translational diffusion coefficient is measured as a function of ionic strength after the removal of H1.

At ionic strength 80 mM NaCl, our results giving a value of -0.60 for b are at variance with those obtained by Osipova et al. [62]. They found $a = 0.55$ indicating a much greater compaction effect than that which we observe. This discrepancy appears to be likely due to the very high salt concentration used (150 mM NaCl).

The small decrease of b (from -0.65 to -0.60) observed here means that the conformation of oligonucleosomes does not change drastically with increasing ionic strength while the rigidness of the chain decreases, due to the folding of linker DNA. Indeed, when the ionic strength is increased from 0 to 80 mM, the translational coefficient of the monomer increases from 2.16×10^{-7} cm^2 s^{-1} to 2.54×10^{-7} cm^2 s^{-1}. By using the lollipop model, this corresponds to a decrease of the DNA tail length of about 125–130 Å. Note that the value of D observed for the H1-depleted monomer at high ionic strength is smaller than that determined in the presence of H1 at low ionic strength (3.02×10^{-7}cm^2 s^{-1}).

The effect of the removal of H1 on the compaction of an oligonucleosomal chain can be estimated by comparison of the present results with those previously reported for H1-containing oligomers [21]. We recall that the experimental dependencies of D on n were

$$D = 3.12 \times 10^{-7} n^{-0.51} \quad (12)$$

at low ionic strength (1 mM phosphate buffer, pH 7.4, 0.2 mM EDTA) and

$$D = 3.12 \times 10^{-7} n^{-0.42} \quad (13)$$

in the presence of 80 mM NaCl. We have to keep in mind that the values of the exponent b were in good accordance with the mean values of the exponent a determined from sedimentation experiments. a was found to be 0.52 [17,23,25,27, 30,61,62,64,65] at low ionic strength and 0.60 [25, 26,62] at high ionic strength.

We see that there is a clear difference in the hydrodynamic behavior of oligonucleosomes containing H1 and depleted of H1. In the presence of H1, the results suggest a helical arrangement of nucleosomes even at low salt concentration and the fact that by increasing the ionic strength, b decreases from -0.51 to -0.42 indicates the formation of supercoiled structures [21]. We analyzed the curves of the friction factor f (eq. 5) vs n (fig. 6). At low ionic strength, data are consistent with a helical structure of 28 nm diameter, 22 nm pitch and 6 nucleosomes, described as lollipops, per turn. As the ionic strength increases, the data can be explained by a decrease in pitch (from 22 to 11 nm) which then agrees with the solenoidal model [8] and a slight decrease in the helical radius. When computations are performed on the H1-depleted oligomeric data, none of the helical models are sufficiently extended to fit the data.

Moreover, we show here that H1-depleted oligomers also condense upon increase of ionic strength but that they do not lead to the characteristic structure exhibited by native oligomers, since b remains equal to -0.60 at 80 mM NaCl. On

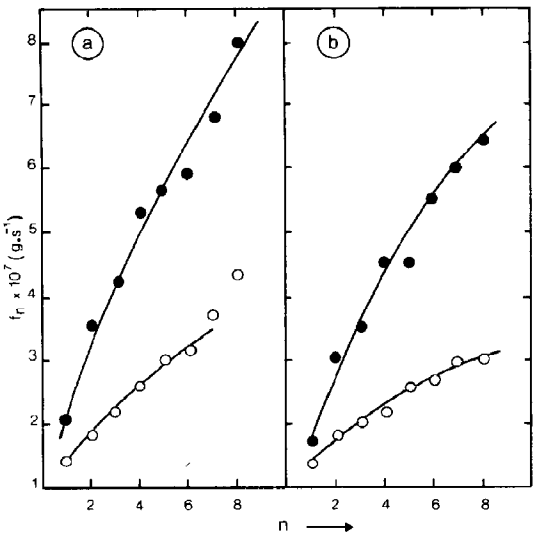

Fig. 6. Dependence of frictional coefficient f_n on the number of nucleosomes in the chain of oligonucleosomes. Salt conditions: (a) 1 mM sodium phosphate buffer, 0.2 mM EDTA, pH 7.4; (b) 1 mM sodium phosphate buffer, 0.2 mM EDTA, 80 mM NaCl, pH 7.4. (○) H1-containing oligonucleosomes, (●) H1-depleted oligonucleosomes.

increasing the ionic strength, the translational coefficient also decreases but its rate of decrease is much smaller for H1-depleted oligomers than for H1-containing oligomers. In the case of stripped oligomers, the condensation may simply arise from the polyelectrolytic behavior of DNA internucleosomal segments.

In conclusion, these results clearly prove that histone H1 is necessary for the formation of a supercoiled structure of oligonucleosomes. We recall that hydrodynamic measurements have provided evidence that a well-defined superstructure of chromatin may exist in low salt conditions [15,17,18,24,30–32,58,60]. The ionic strength-induced condensation of chromatin is thus 'accordion-like' [24,32] making possible the fast reversible loosening of superstructure occurring during the cell cycle. Presently, it is not known how H1 brings about the condensation of extended structures into compact fibers. We can only suggest various possibilities, as the ionic strength increases [24,66]: neighboring H1 may interact with each other or H1 may interact with the DNA of more than one nucleosome or linker region. One can also imagine that H1 may modify the conformation of the spacer, constraining the nucleosomal chains into a more compact particle.

One also has to keep in mind that a condensation very similar to the salt-induced folding of native chromatin has been observed in reconstitution experiments [12,54]. We have indeed recently shown that H1-depleted chromatin reassociated with various H1 subfractions produces fibers more compact than the native ones although some features of native chromatin (CD spectra, thermal denaturation profiles, electron micrographs and nuclease digestion barriers) are correctly restored [54].

References

1 P.J.G. Butler, Crit. Rev. Biochem. 15 (1983) 57.
2 I.L. Cartwright, S.M. Abmayr, G. Fleischmann, K. Lowenhaupt, S.C.R. Elgin, M.A. Keene and G.C. Howard, Crit. Rev. Biochem. 13 (1982) 1.
3 H.G. Davies, J. Cell. Sci. 3 (1968) 129.
4 H. Ris and D.F. Kubai, Annu. Rev. Genet. 4 (1970) 263.
5 K. Brasch, Exp. Cell Res. 101 (1976) 396.
6 P. Labhart, T. Koller and H. Wunderli, Cell 30 (1982) 115.
7 J.P. Langmore and J.R. Paulson, J. Cell Biol. 96 (1983) 1120.
8 J.T. Finch and A. Klug, Proc. Natl. Acad. Sci. U.S.A. 73 (1976) 1897.
9 M. Renz, P. Nehls and J. Hozier, Proc. Natl. Acad. Sci. U.S.A. 74 (1977) 1879.
10 F. Thoma and T. Koller, Cell 12 (1977) 101.
11 F. Thoma, T. Koller and A. Klug, J. Cell Biol. 83 (1979) 403.
12 F. Thoma and T. Koller, J. Mol. Biol. 149 (1981) 709.
13 R.T. Simpson, Biochemistry 17 (1978) 5524.
14 V.C. Littau, C.J. Burdick, V.G. Allfrey and A.E. Mirsky, Proc. Natl. Acad. Sci. U.S.A. 54 (1965) 1204.
15 E.M. Bradbury, B.G. Carpenter and H.W.E. Rattle, Nature 241 (1973) 123.
16 M.A. Billett and J.M. Barry, Eur. J. Biochem. 49 (1974) 477.
17 C. Marion and B. Roux, Nucleic Acids Res. 5 (1978) 4431.
18 B. Roux, C. Marion and J.C. Bernengo in: Electro-optics and dielectrics of macromolecules and colloids, ed. B.R. Jennings (Plenum Press, New York, 1979) p. 163.
19 C. Marion and B. Roux, Biochem. Biophys. Res. Commun. 94 (1980) 535.
20 J.C. Bernengo, P. Bezot, C. Bezot, B. Roux and C. Marion, Ber. Bunsenges. Phys. Chem. 85 (1981) 657.
21 C. Marion, P. Bezot, C. Hesse-Bezot, B. Roux and J.C. Bernengo, Eur. J. Biochem. 120 (1981) 169.

22 C. Marion, L. Pallotta and B. Roux, Biochem. Biophys. Res. Commun. 108 (1982) 1551.
23 G. Mithieux, B. Roux and C. Marion, Biophys. Chem. 20 (1984) 111.
24 C. Marion, J. Biomol. Struct. Dyn. 2 (1984) 303.
25 P.J.G. Butler and J.O. Thomas, J. Mol. Biol. 140 (1980) 505.
26 D.L. Bates, P.J.G. Butler, E.C. Pearson and J.O. Thomas, Eur. J. Biochem. 119 (1981) 469.
27 E.C. Pearson, P.J.G. Butler and J.O. Thomas, EMBO J. 2 (1983) 1367.
28 L.A. Bolund and E.W. Johns, Eur. J. Biochem. 35 (1973) 546.
29 V.C. Gordon, C.M. Knobler, D.E. Olins and V.N. Schumaker, Proc. Natl. Acad. Sci. U.S.A. 75 (1978) 660.
30 B.R. Ramsay-Shaw and K.S. Schmitz, Biochem. Biophys. Res. Commun. 73 (1976) 224.
31 K.S. Schmitz and B.R. Ramsay-Shaw, Biopolymers 16 (1977) 2619.
32 B.R. Ramsay-Shaw and K.S. Schmitz, in: Chromatin structure and function, ed. C.A. Nicolini (Plenum Corp., New York, 1979) p. 427.
33 E. Hantz, A. Cao, E. Taillandier, P. Tivant, M. Drifford, N. Defer and J. Kruh, Biochimie 63 (1981) 891.
34 K.S. Schmitz, N. Parthasarathy, J.C. Kent and J. Gauntt, Biopolymers 21 (1982) 1365.
35 K.S. Schmitz, Biopolymers 21 (1982) 1383.
36 E. Hantz, A. Cao, E. Taillandier, P. Tivant, M. Drifford, N. Defer and J. Kruh, Int. J. Biol. Macromol. 5 (1983) 130.
37 D.R. Hewish and L.A. Burgoyne, Biochem. Biophys. Res. Commun. 52 (1973) 504.
38 J.T. Finch, M. Noll and R.D. Kornberg, Proc. Natl. Acad. Sci. U.S.A. 72 (1975) 3320.
39 U.E. Loening, Biochem. J. 102 (1967) 251.
40 S. Panyim and R. Chalkley, Arch. Biochem. Biophys. 130 (1969) 337.
41 P. Bezot, C. Hesse-Bezot, N. Ostrowsky and B. Quentrec, Mol. Phys. 39 (1980) 549.
42 G. de Murcia, G.C. Das, M. Erard and M. Daune, Nucleic Acids Res. 5 (1978) 523.
43 R.L. Rill, in: Molecular genetics, part III, ed. J.H. Taylor (Academic Press, New York, 1979) p. 247.
44 J.J. Lawrence, D.C.F. Chan and L.H. Piette, Nucleic Acids Res. 3 (1976) 2879.
45 L.J. Kaplan, R. Bauer, E. Morrison, T.A. Langan and G.D. Fasman, J. Biol. Chem. 259 (1984) 8777.
46 A.W. Fulmer and G.D. Fasman, Biopolymers 18 (1979) 2875.
47 A.W. Fulmer and G.D. Fasman, Biochemistry 18 (1979) 659.
48 A.R. McCleary and G.D. Fasman, Arch. Biochem. Biophys. 201 (1980) 603.
49 M.K. Cowman and G.D. Fasman, Biochemistry 19 (1980) 532.
50 K. Watanabe and K. Iso, J. Mol. Biol. 151 (1981) 143.
51 M. Erard, J. Pouyet, A. Mazen, M. Champagne and M. Daune, Biophys. Chem. 14 (1981) 123.
52 C. Marion, B. Roux and P.R. Coulet, FEBS Lett. 157 (1983) 317.
53 C. Marion, B. Roux, L. Pallotta and P.R. Coulet, Biochem. Biophys. Res. Commun. 114 (1983) 1169.
54 J. Roche, C. Marion, C. Gorka, B. Roux and J.J. Lawrence, Biochem. Biophys. Res. Commun. 121 (1984) 530.
55 F. Chauvin, B. Roux and C. Marion, J. Biomol. Struct. Dyn. 2 (1985) 805.
56 J. Ausio, N. Borochov, D. Seger and H. Eisenberg, J. Mol. Biol. 177 (1984) 373.
57 C.R. Cantor and P.J. Schimmel, Biophysical chemistry (W.F. Freeman, San Francisco, 1980) p. 1027.
58 A.M. Campbell, R.I. Cotter and J.F. Pardon, Nucleic Acids Res. 5 (1978) 1571.
59 P. Suau, E.M. Bradbury and J.P. Baldwin, Eur. J. Biochem. 97 (1979) 593.
60 L. Perez-Grau, J. Bordas and M.H.J. Koch, Nucleic Acids Res. 12 (1984) 2987.
61 M. Noll and R.D. Kornberg, J. Mol. Biol. 109 (1977) 393.
62 R.N. Osipova, V.A. Pospelov, S.B. Svetlikova and V.I. Vorob'ev, Eur. J. Biochem. 113 (1980) 183.
63 J. Garcia de la Torre and V.A. Bloomfield, Biopolymers 16 (1977) 1747.
64 J.M. Gottesfeld and P.J.G. Butler, Nucleic Acids Res. 4 (1977) 3155.
65 J.O. Thomas and P.J.G. Butler, J. Mol. Biol. 144 (1980) 89.
66 W.H. Strätling, Biochemistry 18 (1979) 596.